Space-Frequency Coded HIPERLAN/2

Celal Esli, *Student Member, IEEE,* Baris Ozgul, *Student Member, IEEE,* and Hakan Delic, *Senior Member, IEEE*

Abstract — *This paper attempts to provide an evaluation of High Performance Local Area Network Type 2 (HIPERLAN/2), equipped with space-frequency coded double-antenna transmit diversity. The HIPERLAN/2 physical layer entities are simulated for frequency-selective fading channels for the standard's digital modulation schemes of BPSK, QPSK, 16-QAM and 64-QAM. Protocol data unit (PDU) error rate comparisons of HIPERLAN/2 with and without space-frequency coding reveal the potential gains and caveats. The analytical bit error probability calculations confirm that the simulation results are consistent with the theory*[1].

Index Terms — OFDM, space-frequency coding, transmitter diversity, wireless LAN.

I. INTRODUCTION

The number of networked homes with personal computers, as well as entertainment devices is approaching 100 millions. It is argued that the connection of consumer-oriented home electronics will have to take place through a local area network (LAN) structure. These so-called "multiservice home networks" are envisioned to be extensions of the wireless LAN standards such as the IEEE 802.11a and the European Telecommunications Standards Institute (ETSI) High Performance Local Area Network Type 2 (HIPERLAN/2) [9].

The HIPERLAN/2 is a system that is designed to give wireless access to the Internet and multimedia applications such as real-time video with data rates up to 54 Mbps. Being a quick and easily set system and providing internetworking with several core networks including the Ethernet, HIPERLAN/2 has many application areas, and features such as high-speed data transmission capability, quality of service support, automatic frequency allocation, mobility and security support and a connection-oriented link.

The HIPERLAN/2 standard is based on orthogonal frequency division multiplexing (OFDM), which is an efficient technology that splits the available bandwidth among several closely spaced, mutually orthogonal subcarriers. Orthogonality avoids multiuser interference (MUI) so long as there is no frequency offset among the subcarriers [5], [6], [15]. Moreover, by transmitting over a number of parallel narrowband channels instead of a single wideband one, the frequency-selective fading problem is transformed into communications over multiple flat fading channels. However, channel nulls can still hamper the OFDM transmissions, and additional measures such as transmit diversity may be taken for reliable high-speed data communication.

In a diversity system, several replicas of the transmitted signal arrive at the receiver. Through careful coordination among transmissions via coding in time or frequency, it is possible to alleviate the destructive effects of channel nulls to a certain extent. By employing multiple spatially separated antennas at the base station, diversity gain can be achieved with no need to increase the size or complexity of the receivers significantly [7].

The benefits of employing transmit diversity in OFDM systems has been under scrutiny recently. The IEEE 802.11a and HIPERLAN/2 standards, coupled with space division multiplexing are shown to yield significant throughput and bit error rate enhancements with multiple antennas [11], [12], [13], [16], [19]. Other multi-input, multi-output wireless OFDM systems in the 2-5 GHz range are also under development [2], [14].

In this paper, the HIPERLAN/2 transceiver structure is equipped with space-frequency coding (SFC) over two transmit antennas. The physical layer of the HIPERLAN/2 standard is simulated in a frequency-selective fading environment with and without SFC, and the potential gains to be achieved through transmit diversity are demonstrated. Doppler spread-related issues are not considered because SFC does not directly combat time-selectivity.

The organization of the paper is as follows. Section II briefly outlines the HIPERLAN/2 physical layer. Space-frequency coded HIPERLAN/2 is described in Section III. Performance analysis of the space-frequency coded HIPERLAN/2 is furnished in Section IV. The simulation model and results are in Section V, including the comparison of analytical and simulation results. Conclusions are drawn in Section VI.

II. THE HIPERLAN/2 PHYSICAL LAYER

The HIPERLAN/2 physical layer functions are shown in Fig. 1. The standard specifies only the transmitter structure. The content of each protocol data unit (PDU) train from the data link control (DLC) layer is scrambled with a 127-bit scrambler to prevent synchronization losses due to long sequences of the same bit value, as well as, to reduce radio interference [4]. The scrambled bits are protected by forward

[1] This work was supported by the Bogazici University Research Projects under Grant No. 03A206.

The authors are with the Department of Electrical and Electronics Engineering, Bogazici University, Bebek 34342 Istanbul, Turkey. (e-mail: {celal.esli, ozgulbar, delic}@boun.edu.tr)

Contributed Paper
Manuscript received July 12, 2004

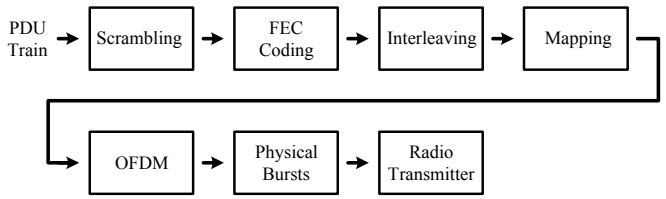

Fig. 1. The transmitter structure in HIPERLAN/2 [4].

error-correction (FEC). Data interleaving is defined by a two-step permutation procedure, where consecutive coded bits are first mapped onto noncontiguous subcarriers. Next, the consecutive coded bits are mapped alternately onto less and more significant bits of the constellation. This approach avoids long runs of low-reliability bits [4].

The 48 OFDM subcarriers are modulated by binary phase shift-keying (BPSK), quadrature PSK (QPSK), 16-ary quadrature amplitude modulation (16-QAM) or 64-QAM constellations depending on the physical (PHY) mode selected for the data transmission rate [2]. The interleaved binary serial input data are grouped into one, two, four or six bits and converted into complex numbers representing the Gray-coded constellation points.

TABLE I
THE HIPERLAN/2 OFDM PARAMETERS [4]

Parameter	Value
Sampling rate $f_s = 1/T$	20 MHz
Useful symbol part duration (T_U)	$64T = 3.2$ μs
Cyclic prefix duration	$16T = 0.8$ μs (Mandatory)
	$8T = 0.4$ μs (Optional)
Symbol interval	$80T = 4.0$ μs
	$72T = 3.6$ μs
Number of data subcarriers	48
Number of pilot subcarriers	4
Total number of subcarriers (N_{ST})	52
Subcarrier spacing (Δf)	$1/T_U = 0.3125$ MHz
Spacing between the two outermost subcarriers	$N_{ST}(\Delta f) = 16.25$ MHz

The system has five kinds of PHY bursts: broadcast downlink, uplink burst with short preamble, uplink burst with long preamble, direct link burst, which is optional. All OFDM symbols contain data in data carriers and reference information in pilot carriers. A cyclic extension of the inverse discrete Fourier transform (IDFT) output, called the cyclic prefix, is appended as a precaution against intercarrier interference (ICI). Equalization is still required at the receiver to overcome residual ICI. Numerical values of the OFDM parameters for the HIPERLAN/2 standard are presented in Table I.

There are five types of standardized channel models for HIPERLAN/2, derived from measurements in typical indoor and outdoor environments with root mean-squared (rms) delay spreads (ds) ranging that lie between 50 to 250 ns. These five models are defined in Table II with parameters rms ds and Rice factor (K). The experimental results in Section V are obtained for model A, which specifies a finite impulse response (FIR) channel model with eight taps and an rms delay spread of 50 ns.

TABLE II
CHANNEL MODELS [3]

Name	RMS DS	K	Environment
A	50 ns	-	Office NLOS
B	100 ns	-	Open space/office NLOS
C	150 ns	-	Large open space NLOS
D	140 ns	10 dB	Large open space LOS
E	250 ns	-	Large open space NLOS

III. SPACE-FREQUENCY CODED HIPERLAN/2

The block diagram of HIPERLAN/2 transmitter and receiver structures equipped with SFC capability is given in Fig. 2. The N data symbols, each with duration T, are fed into a serial-to-parallel converter to generate the nth OFDM block of duration NT, which is denoted by $\mathbf{S}(n)$ [3].

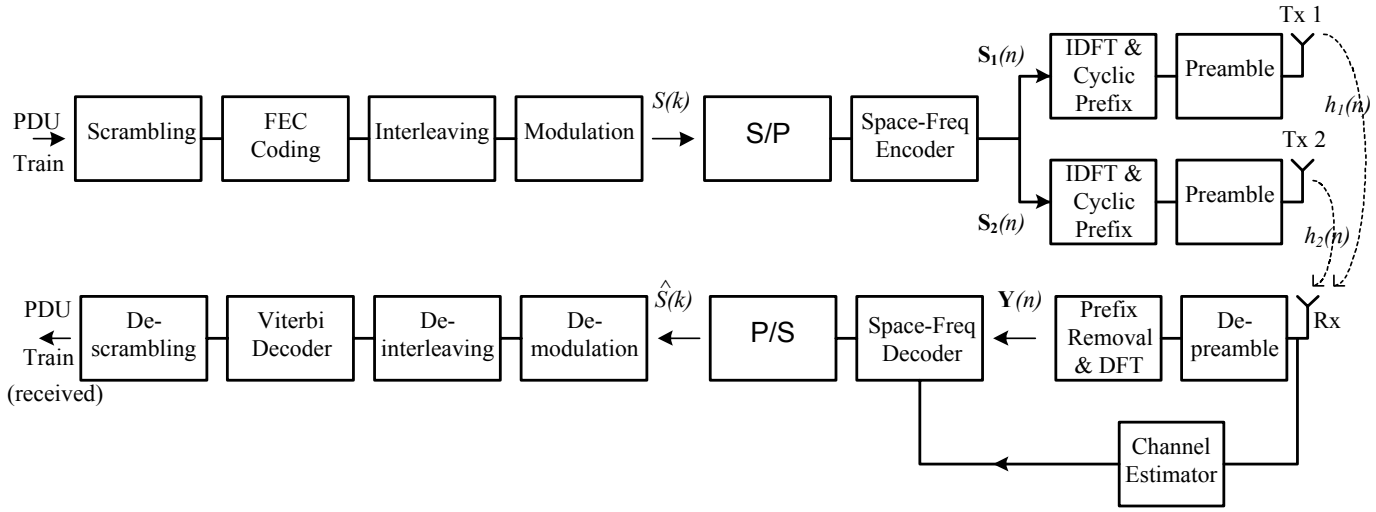

Fig. 2. Block diagram of HIPERLAN/2 with space-frequency coded double-transmit antenna diversity. In the figure, $\mathbf{S}_1(n)$ and $\mathbf{S}_2(n)$ are the nth coded OFDM blocks, and $\mathbf{Y}(n)$ is the corresponding received OFDM block.

$$\mathbf{S}(n) = \left[S_0(n)\ S_1(n) \ldots\ S_{N-2}(n)\ S_{N-1}(n) \right],$$

where $S_m(n) := S(nN+m)$, $m = 0, 1, ..., N-1$, denote the mth symbol of the nth data block.

Using the nth OFDM block $\mathbf{S}(n)$, the space-frequency encoder generates the two data vectors [7]

$$\mathbf{S}_1(n) = \left[S_0(n)\ -S_1^*(n) \ldots\ S_{N-2}(n)\ -S_{N-1}^*(n) \right]^T$$
$$\mathbf{S}_2(n) = \left[S_1(n)\ \ S_0^*(n) \ldots\ S_{N-1}(n)\ \ S_{N-2}^*(n) \right]^T$$

Before transmission, IDFT is applied to both vectors and cyclic prefixes are appended. Subsequently, $\mathbf{S}_1(n)$ and $\mathbf{S}_2(n)$ are simultaneously transmitted over the respective antennas which are positioned such that the corresponding channels are uncorrelated. At the receiver, following the cyclic prefix removal, discrete Fourier transform (DFT) is applied.

The N-point DFTs of channel impulse responses $h_1(n)$ and $h_2(n)$, which are assumed to stay constant for the duration of the block, have the channel transfer functions $H_{1,0}(n)$, $H_{1,1}(n)$, . . . , $H_{1,N-1}(n)$ and $H_{2,0}(n)$, $H_{2,1}(n)$, . . ., $H_{2,N-1}(n)$, respectively, at the N subcarriers. Ignoring the OFDM block index n for simplicity, the received symbols are

$$\begin{aligned} Y_m &= H_{1,m}S_m + H_{2,m}S_{m+1} + Z_m, \\ Y_{m+1} &= -H_{1,m+1}S_{m+1}^* + H_{2,m+1}S_m^* + Z_{m+1}, \end{aligned} \tag{1}$$

for $m = 0, 2, 4, . . ., N-2$, where Z_m represents the zero mean, complex, additive white Gaussian noise (AWGN) term for the mth received symbol. Rearranging (1),

$$\begin{bmatrix} Y_m \\ Y_{m+1}^* \end{bmatrix} = \mathbf{H} \begin{bmatrix} S_m \\ S_{m+1} \end{bmatrix} + \begin{bmatrix} Z_m \\ Z_{m+1}^* \end{bmatrix}, \tag{2}$$

where

$$\mathbf{H} = \begin{bmatrix} H_{1,m} & H_{2,m} \\ H_{2,m+1}^* & -H_{1,m+1}^* \end{bmatrix}, \tag{3}$$

and (3) represents Alamouti-type zero-forcing decoding of SFC. Assuming perfect channel state information at the receiver, the space-frequency decoder generates the decision estimates through [1]

$$\begin{bmatrix} \hat{S}_m \\ \hat{S}_{m+1} \end{bmatrix} = \mathbf{H}^H\mathbf{H} \begin{bmatrix} S_m \\ S_{m+1} \end{bmatrix} + \mathbf{H}^H \begin{bmatrix} Z_m \\ Z_{m+1}^* \end{bmatrix} \tag{4}$$

where the superscript H is the conjugate transpose. The matrix product $\mathbf{H}^H\mathbf{H}$ in (4) is

$$\mathbf{H}^H\mathbf{H} = \begin{bmatrix} H_{11} & H_{12} \\ H_{21} & H_{22} \end{bmatrix},$$

where, for $m = 0, 2, 4, . . . , N-2$, [7]

$$H_{11} = \left|H_{1,m}\right|^2 + \left|H_{2,m+1}\right|^2, \tag{5}$$
$$H_{12} = H_{1,m}^* H_{2,m} - H_{2,m+1}H_{1,m+1}^*, \tag{6}$$
$$H_{21} = H_{2,m}^* H_{1,m} - H_{1,m+1}H_{2,m+1}^*, \tag{7}$$
$$H_{22} = \left|H_{2,m}\right|^2 + \left|H_{1,m+1}\right|^2. \tag{8}$$

For both transmit antennas, the data symbols in the corresponding OFDM symbol vectors are transmitted on adjacent subcarriers. It is assumed that contiguous subcarriers are highly correlated, i.e., $H_{1,m} \approx H_{1,m+1}$ and $H_{2,m} \approx H_{2,m+1}$, so that (5) and (6) are approximately zero. Since $\mathbf{H}^H\mathbf{H}$ becomes a diagonal matrix, S_m and S_{m+1} in (4) can then be estimated separately.

IV. Performance Analysis of SFC-HIPERLAN/2

A. Analysis of M-QAM OFDM System

Assuming that the channel induced errors in the cyclic prefix introduces negligible degradation, the approximate uncoded bit error probability expression for M-QAM with Gray mapping over frequency-selective fading is given by [14]

$$P_b^{M-QAM} \approx \frac{0.2}{N} \sum_{k=0}^{N-1} \exp\left(-\frac{1.6\gamma_s \left|H_k\right|^2}{2^\beta - 1} \right) \tag{9}$$

where β is bits per symbol, $M = 2^\beta$, N is the number of subcarriers and γ_s is the symbol-to-noise energy ratio (SNR) at the transmitter.

Expression for the average bit error probability for OFDM with M-QAM modulation can be written as

$$\overline{P}_b^{M-QAM} = \int_0^\infty P_b^{M-QAM}\, p(\gamma) d\gamma \tag{10}$$

where $p(\gamma)$ is the probability density function of $\gamma = \gamma_s|H_k|^2$.

Since γ is chi-square distributed function, $p(\gamma)$ is represented as

$$p(\gamma) = \frac{1}{\overline{\gamma}} \exp\left(-\frac{\gamma}{\overline{\gamma}} \right) \tag{11}$$

where $\overline{\gamma} = \gamma_s \mathrm{E}\{|H_k|^2\}$ and $\mathrm{E}\{|H_k|^2\}$ is the expectation of $|H_k|^2$.

B. Analysis of Uncoded SFC-OFDM System with M-QAM

To derive the bit error probability expression for the SFC system, SNR (γ) at the SFC decoder should be defined at first. From (4) and the conclusion that $\mathbf{H}^H\mathbf{H}$ is a diagonal matrix, decision estimates can be written as

$$\hat{S}_m = H_{11}S_m + H_{1,m}^* Z_m + H_{2,m+1}Z_{m+1}^*, \tag{12}$$
$$\hat{S}_{m+1} = H_{22}S_{m+1} + H_{2,m}^* Z_m + H_{1,m+1}Z_{m+1}^*, \tag{13}$$

where m=0, 2, 4, …, N-2. Through (10) and (11), the SNR at the SFC decoder is

$$SNR_m = \frac{\left|H_{11}\right|^2}{\left|H_{1,m}\right|^2 + \left|H_{2,m+1}\right|^2} \frac{E_s}{N_0}, \tag{14}$$

$$SNR_{m+1} = \frac{\left|H_{22}\right|^2}{\left|H_{2,m}\right|^2 + \left|H_{1,m+1}\right|^2} \frac{E_s}{N_0}, \tag{15}$$

where E_s is the symbol energy and N_0 is the one-sided noise power spectral density. Equations (14) and (15) together with (5) and (8) respectively, give the final SNR expressions:

$$SNR_m = \left(\left|H_{1,m}\right|^2 + \left|H_{2,m+1}\right|^2 \right) \frac{E_s}{N_o}, \tag{16}$$

$$SNR_{m+1} = \left(\left|H_{2,m}\right|^2 + \left|H_{1,m+1}\right|^2 \right) \frac{E_s}{N_o}. \tag{17}$$

The bit error probability expression for SFC-OFDM system with *M*-QAM modulation can be approximated as [13]

$$P_b^{SFC,M-QAM} \approx \frac{0.2}{N} \sum_{k=0}^{N-1} \exp\left(-\frac{1.6 \sum_{i=1}^{M_T} \tilde{\gamma}_{i,k}}{2(2^\beta - 1)} \right) \tag{18}$$

where $\tilde{\gamma}_{i,k}$ is the SNR at *k*th subchannel through the *i*th antenna. To obtain the uncoded bit error probability for SFC-OFDM with *M*-QAM modulation, equation (18) and the SNR values from (16) and (17) are combined. The resulting expression can be written as

$$\begin{aligned} P_b^{SFC,M-QAM} \approx \\ \frac{0.2}{N} \Bigg[& \exp\left(-\frac{1.6\gamma_s \left(\left|H_{1,0}\right|^2 + \left|H_{2,1}\right|^2 \right)}{2(2^\beta - 1)} \right) + \exp\left(-\frac{1.6\gamma_s \left(\left|H_{1,1}\right|^2 + \left|H_{2,0}\right|^2 \right)}{2(2^\beta - 1)} \right) \\ & + \exp\left(-\frac{1.6\gamma_s \left(\left|H_{1,2}\right|^2 + \left|H_{2,3}\right|^2 \right)}{2(2^\beta - 1)} \right) + \exp\left(-\frac{1.6\gamma_s \left(\left|H_{1,3}\right|^2 + \left|H_{2,2}\right|^2 \right)}{2(2^\beta - 1)} \right) + \ldots \\ & + \exp\left(-\frac{1.6\gamma_s \left(\left|H_{1,N-2}\right|^2 + \left|H_{2,N-1}\right|^2 \right)}{2(2^\beta - 1)} \right) + \exp\left(-\frac{1.6\gamma_s \left(\left|H_{1,N-1}\right|^2 + \left|H_{2,N-2}\right|^2 \right)}{2(2^\beta - 1)} \right) \Bigg] \end{aligned} \tag{19}$$

The average uncoded bit error probability for SFC-OFDM with *M*-QAM is

$$\overline{P}_b^{SFC,M-QAM} = \int_0^\infty \int_0^\infty P_b^{SFC,M-QAM} p(\gamma_1) p(\gamma_2) d\gamma_1 d\gamma_2 \tag{20}$$

where $\gamma_i = \gamma_s \left|H_{i,k}\right|^2$, i=1,2, and $p(\gamma_i)$ is the probability density function,

$$p(\gamma_i) = \frac{1}{\overline{\gamma}_i} \exp\left(-\frac{\gamma_i}{\overline{\gamma}_i} \right). \tag{21}$$

Finally, the uncoded average bit error probability for the SFC-OFDM system with double antennas and *M*-QAM under frequency selective fading is obtained by substituting (19) and (21) into (20):

$$\overline{P}_b^{SFC,M-QAM} \approx \frac{0.2}{\left(1 + \frac{0.31\left(E/N_0\right)}{2\left(2^\beta - 1\right)} \right)^2} \tag{22}$$

where channels with eight tap weights that are statistically independent and that have zero-mean complex Gaussian distribution and exponentially decaying power profile are assumed.

The bit error probability expression for OFDM with *M*-PSK modulation can be found in a similar fashion as [16]

$$P_b^{M-PSK} \approx \frac{0.2}{N} \sum_{k=0}^{N-1} \exp\left(-\frac{7\gamma_s \left|H_k\right|^2}{2^{1.9\beta} + 1} \right)$$

with the same calculations as those for the *M*-QAM case. The resulting uncoded average bit error probability expression for SFC-OFDM system with double antennas and *M*-PSK under frequency-selective fading is

$$\overline{P}_b^{SFC,M-PSK} \approx \frac{0.2}{\left(1 + \frac{1.34\left(E/N_0\right)}{2\left(2^{1.9\beta} + 1\right)} \right)^2}. \tag{23}$$

C. Analysis of Coded SFC-OFDM System

The HIPERLAN/2 standard uses rate-½ convolutional code with generators (133,171) [4]. To derive the coded bit error probability of SFC-HIPERLAN/2, the following bit error probability bound will be used with the assumption that the channel error probabilities are low enough [8].

$$P_b(E) < \frac{1}{k} B_{d_{free}} 2^{d_{free}} p^{d_{free}/2} \tag{24}$$

where k is the number of information bits per unit time, d_{free} is the minimum weight code word of any length produced by a nonzero information sequence [18], $B_{d_{free}}$ is the total number of nonzero information bits on all weight d_{free} paths and p is the uncoded bit error probability. $B_{d_{free}}$ and d_{free} are equal to 36 [8] and 10 [18], respectively. The final bir error probability expression for the SFC-HIPERLAN/2 can be found by substituting the p values (22) or (23) into (24).

V. Simulations and Discussion

A. Simulation Model

The effectiveness of SFC on the PDU error rate (PER) performance of the HIPERLAN/2 standard is evaluated. All simulations operate at the baseband. The performance of HIPERLAN/2 with and without SFC is tested for the broadcast physical layer burst in a frequency-selective channel contaminated by zero-mean, complex AWGN. Each digital modulation scheme prescribed by HIPERLAN/2, namely BPSK, QPSK, 16-QAM and 64-QAM, is averaged over 40 randomly generated, distinct channels for the E_b/N_0 = 0-20 dB range. After inserting the SFC block into the HIPERLAN/2 configuration, all the simulations are repeated for all modulation techniques, E_b/N_0 values (which are now normalized so that the same total signal-to-noise ratio is maintained), and 20 distinct channel pairs. The Monte Carlo simulations are run for 500,000 and 200,000 bits each for the BPSK/QPSK and 16/64-QAM modes, respectively. All results are obtained for user PDUs, which consist of 54 bytes.

As stated in Section II, channel model A is used through simulations. The channel tap weights are statistically independent and have zero-mean complex Gaussian distribution, with exponentially decaying power profile. Perfect channel estimation and synchronization are assumed.

For the sake of simplicity in the FEC coding part, a convolutional encoder of rate 1/2 is used throughout, even though HIPERLAN/2 demands puncturing for the QAM modes to match the 27-, 36- and 54-Mbps PHY bit rates. Decoding is accomplished through the Viterbi algorithm. The interleaver takes 48-bit blocks of data.

B. Simulation Results

Simulation results that reflect the PER versus E_b/N_0 performance for the HIPERLAN/2 modulation alternatives are displayed in Figures 3-6. There is an overall agreement with the PER figures reported in [5]. In particular, Fig. 3 depicts the averages of BPSK and QPSK experiments, which respectively correspond to 6 and 12 Mbps PHY layer bit rates with rate-1/2 convolutional coding.

On average, SFC offers about two orders of magnitude of PER improvement at around E_b/N_0 = 10 dB. Past E_b/N_0 = 10 dB, PER values that are even below 1×10^{-4} are attainable using SFC. This trend is consistent with the fact that diversity gain really kicks in at high SNRs.

For specific channel realizations, SFC may do better or worse than the average. The channel pair with the following FIR filter coefficients illustrates the potential gain that can be harvested with SFC.

$$\begin{aligned} h_1 = [&0.4127 + j0.1026 \quad 0.4814 - j0.1851 \\ &0.0137 - j0.2870 \quad -0.1174 - j0.0156 \\ &-0.1237 + j0.0293 \quad -0.0104 + j0.0596 \\ &0.0337 + j0.0327 \quad 0.0064 - j0.0189], \end{aligned} \tag{25}$$

$$\begin{aligned} h_2 = [&-1.4204 - j1.0088 \quad 0.0676 - j0.1302 \\ &0.1801 - j0.0578 \quad 0.1849 + j0.0991 \\ &-0.0318 + j0.0262 \quad 0.0500 + j0.1097 \\ &-0.0139 - j0.0080 \quad 0.0222 + j0.0378]. \end{aligned} \tag{26}$$

Of the two channels, h_1 undergoes severe signal losses while h_2 enjoys relatively good health. Under the conditions depicted by (7) and (8), the PER behavior is similar to that observed when averaged over randomly generated channels (see Fig. 4).

The SFC decoding procedure, which linearly combines the gains of the two channels when contiguous subcarriers are used, relies on h_2 for symbol recovery. In Fig. 4, the results without SFC reflect the HIPERLAN/2 performance under the "bad" channel, h_1. One can readily observe the degree of improvement SFC can supply when at least one transmission path does not experience a null.

In the 16-QAM and 64-QAM modes, which are employed for high-rate data communication, SFC does not appear to offer much of an advantage on the average (Fig. 5).

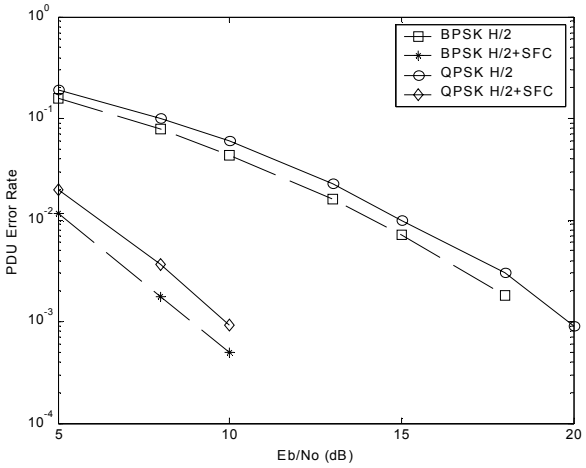

Fig. 3. Simulation results of PDU error rates for BPSK and QPSK, averaged over 40 channels without SFC, and over 20 channel pairs with SFC (HIPERLAN/2 channel A).

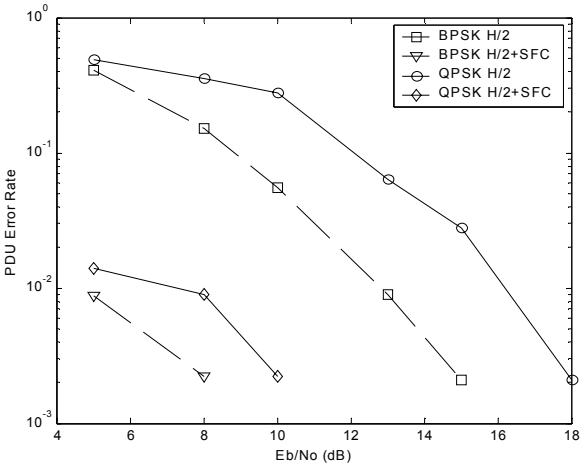

Fig. 4. Simulation results of PDU error rates for BPSK and QPSK, with and without SFC through channels (25) and (26) (HIPERLAN/2 channel A).

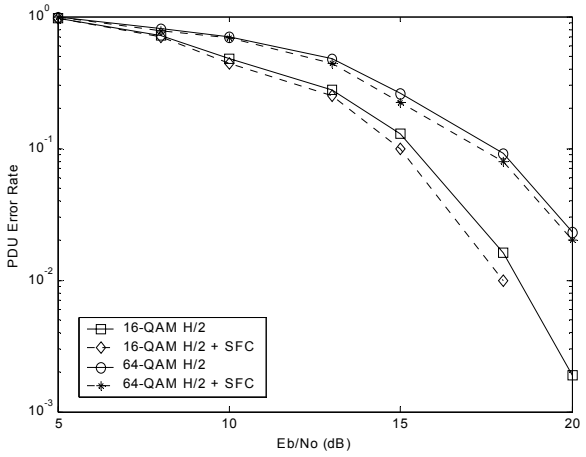

Fig. 5. Simulation results of PDU error rates for 16-QAM and 64-QAM, averaged over 40 channels without SFC, and over 20 channel pairs with SFC (HIPERLAN/2 channel A).

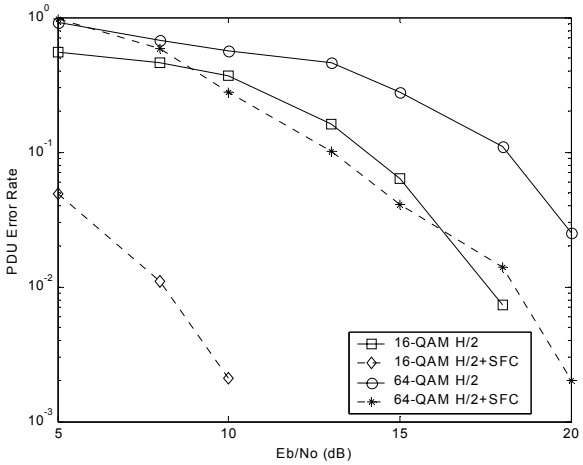

Fig. 6. Simulation results of PDU error rates for 16-QAM and 64-QAM, with and without SFC through channels (25) and (26) (HIPERLAN/2 channel A).

C. Comparison of Analytical and Simulated Results

Comparison of analytical and simulated results that reflect the BER versus E_b/N_0 performances for the SFC-HIPERLAN/2 are displayed in Figures 7 and 8 for QPSK and 16-QAM, respectively. Theoretical results are obtained through (23), (24), and (25). In both figures, the E_b/N_0 range is selected in

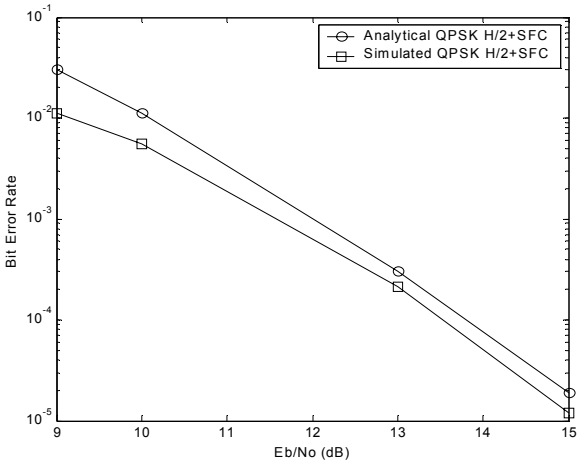

Fig. 7. Bit error rates for analytical and simulated QPSK with SFC.

accordance with the assumptions in the theoretical analysis. As expected, the analytical approximations do not give satisfactory results at low E_b/N_0, whereas they provide upper bounds that are consistent with the simulated results at high E_b/N_0 values. Therefore, we conclude that the simulation experiments are reliable and verifiable by mathematical analysis.

VI. CONCLUSION

Double-antenna transmit diversity with space-frequency coding offers an efficient way to improve the performance of the HIPERLAN/2 protocol suite, especially in the BPSK/QPSK modes. The effectiveness of the diversity scheme

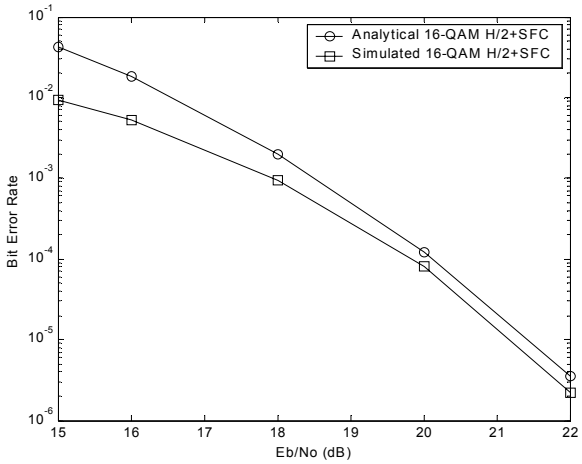

Fig. 8. Bit error rates for analytical and simulated 16-QAM with SFC.

depends on the FIR channel characteristics. When at least one antenna path does not suffer much from channel nulls, HIPERLAN/2 with SFC enjoys substantially lower PER at lower bit rates.

As the number of constellation points increases, there is a degradation in the performance enhancement supplied by the SFC algorithm. While for specific channels, SFC may have a lot to offer for 64-QAM, the average performance improvement turns out to be minor. This outcome is due to those cases where both channels are destructive. In addition, the physical layer structure of the HIPERLAN/2 standard imposes certain limitations. For instance, just 48 subcarriers may not transform the frequency selective nature of the channel into sufficiently flat, parallel ones. Moreover, the rate-9/16 and rate-3/4 convolutional codes do not seem to be adequate in handling the errors that occur with 16-QAM and 64-QAM constellations.

Finally, while HIPERLAN/2 is considered here, its physical layer is very similar to that of the 5-GHz IEEE 802.11a, and the conclusions of this paper apply to the latter standard, as well.

REFERENCES

[1] S. M. Alamouti, "A simple transmitter diversity scheme for wireless communications", *IEEE Journal on Selected Areas in Communications*, Vol. 16, No. 8, pp. 1451-1458, October 1998.

[2] M. D. Batariere, J. F. Kepler, T. P. Krauss, S. Mukthavaram, J. W. Porter and F. W. Vook, "An experimental OFDM system for broadband mobile communications", *Proceedings of the 54th IEEE Vehicular Technology Conference, Vol. 4*, Atlantic City, USA, October 2001, pp. 1947- 1951.

[3] U. Dettmar, J. Khun-Jush, P. Schramm, J. Thielecke, and U. Wachsmann, "Modulation for HIPERLAN type 2", *Proceedings of the 49th IEEE Vehicular Technology Conference, Vol. 2*, Houston, USA, May 1999, pp. 1094-1100.

[4] ETSI TS 101 475 V 1.3.1, *Broadband Radio Access Networks (BRAN): HIPERLAN Type 2; Physical (PHY) Layer*, 2001.

[5] J. Khun-Jush, P. Schramm, U. Wachsmann and F. Wenger, "Structure and performance of the HIPERLAN/2 physical layer", *Proceedings of the 50th IEEE Vehicular Technology*

Conference, Vol. 5, Amsterdam, The Netherlands, September 1999, pp. 2667-2671.

[6] J. Khun-Jush, P. Schramm, G. Malmgren and J. Torsner, "HiperLAN2: broadband wireless communications at 5 GHz", *IEEE Communications Magazine*, Vol. 40, No. 6, pp. 130-136, June 2002.

[7] K. Lee and D. B. Williams, "A space-frequency transmitter diversity technique for OFDM systems", *Proceedings of the IEEE GLOBECOM, Vol. 3*, San Francisco, USA, November 2000, pp. 1473-1477.

[8] S. Lin and D.J. Costello, *Error Control Coding*, New Jersey, USA: Prentice-Hall, 1983.

[9] B. McFarland, G. Chesson, C. Temme and T. Meng, "The 5-UP protocol for unified multiservice wireless networks", *IEEE Communications Magazine*, Vol. 39, No. 11, pp. 74-80, November 2001.

[10] J. Medbo and P. Schramm, *Channel Models for HIPERLAN 2*, ETSI/BRAN Document No. 3ERI085B, 1998.

[11] J.-H. Moon, Y.-H. You, W.-G. Jeon, K.-W. Kwon and H.-K. Song, "Peak-to-average power control for multiple-antenna HIPERLAN/2 and IEEE802.11a systems", *IEEE Transactions on Consumer Electronics*, Vol. 49, No. 4, pp. 1078-1083, November 2003.

[12] R. J. Piechocki, A. R. Nix, C. N. Canagarajah and J. P. McGeehan, "Performance evaluation of BLAST-OFDM enhanced HIPERLAN/2 using simulated and measured channel data", *IEE Electronics Letters*, Vol. 37, No. 18, pp. 1137-1139, August 2001.

[13] R. Piechocki, P. Fletcher, A. Nix, N. Canagarajah and J. McGeehan, "A measurement based feasibility study of space-frequency MIMO detection and decoding techniques for next generation wireless LANs", *IEEE Transactions on Consumer Electronics*, Vol. 48, No. 3, pp. 732-737, August 2002.

[14] H. Sampath, S. Talwar, J. Tellado, V. Erceg and A. Paulraj, "A fourth-generation MIMO-OFDM broadband wireless system: design, performance, and field trials", *IEEE Communications Magazine*, Vol. 40, No. 9, pp. 143-149, September 2002.

[15] R. van Nee and R. Prasad, *OFDM for Wireless Multimedia Communications*, Boston, USA: Artech House, 2000.

[16] A. van Zelst and T. C. W. Schenk, "Implementation of a MIMO OFDM-based wireless LAN system", *IEEE Transactions on Signal Processing*, Vol. 52, No. 2, pp. 483-494, February 2004.

[17] M. Torabi and M.R. Soleymani, "Performance evaluation of space-frequency coded OFDM systems over frequency selective fading channels", *Proceedings of the IEEE Canadian Conference on Electrical and Computer Engineering, Vol. 3*, Montreal, Canada, pp. 1699-1702, May 2003.

[18] Z. Wang, S. Zhou and G. B. Giannakis, "Joint coding-precoding with low-complexity turbo-decoding", *IEEE Transactions on Wireless Communications*, Vol. 3, No. 3, pp. 832-842, May 2004.

[19] Q. Xuemei, M. Ghosh and J. P. Meehan, "Optimal antenna diversity combining for IEEE 802.11a system", *IEEE Transactions on Consumer Electronics*, Vol. 48, No. 3, pp. 738-742, August 2002.

Celal Esli (M'03) was born in Istanbul, Turkey, in 1981. He received the B.S. degree (with honors) in electrical and electronics engineering from Bogazici University, Istanbul, Turkey, in July 2003. He is currently enrolled as a M.S. student in electrical and electronics engineering at Bogazici University. His research interests are in the broad area of wireless communications.

Barış Ozgul (M'98) received the B.S. and M.S. degrees in electrical and electronics engineering, from Bogazici University, Istanbul, Turkey, in 1998 and 2002, respectively. From 1998 to 2003, he worked in Nortel Networks/Netas, as a software architect. He joined Turkcell Iletisim Hizmetleri A.S. in 2003. Currently, he is pursuing the Ph.D. degree in the Department of Electrical and Electronics Engineering, Bogaziçi University. His research interests include signal processing and communications, with emphasis on wireless multiple access and the physical layer problems in wireless communications.

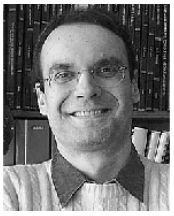

Hakan Delic (S'88–M'93–SM'00) received the B.S. degree (with honors) in electrical and electronics engineering from Bogazici University, Istanbul, Turkey, in 1988, and the M.S. and the Ph.D. degrees in electrical engineering from the University of Virginia, Charlottesville, in 1990 and 1992, respectively.

He was a Research Associate with the University of Virginia Health Sciences Center from 1992 to 1994. In September 1994, he joined the University of Southwestern Louisiana, Lafayette, where he was on the Faculty of the Department of Electrical and Computer Engineering until February 1996. He was a Visiting Associate Professor in the Department of Electrical and Computer Engineering, University of Minnesota, Minneapolis, during the 2001–2002 academic year. He is currently a professor of electrical and electronics engineering at Bogazici University. His research interests lie in the areas of communications and signal processing. His current research focuses on wireless multiple access, application of signal processing techniques to wireless networking, iterative decoding, robust systems, and sensor networks. He frequently serves as a consultant to the telecommunications industry.